

# **A Fully Digital Hysteresis Current Controller for an Active Power Filter**

David M.E. Ingram and Simon D. Round

Department of Electrical & Electronic Engineering

University of Canterbury

Private Bag 4800

Christchurch, New Zealand

*Abstract* An active power filter is used to eliminate current harmonics produced by non-linear loads. This paper discusses a fully digital method of controlling a power inverter used to inject the active filter compensating currents into the power system. A digital signal processor performs the harmonic isolation and generates a digital reference current. A hysteresis current controller has been implemented in a field programmable gate array that generates the inverter switching signals using this reference. This reduces the analogue circuitry and enhances the system's immunity to EMI. The performance of a small-scale inverter under completely digital control is presented and discussed.

# 1. Introduction

## 1.1 The Active Power Filter

Current harmonics produced by non-linear loads, such as switching power supplies and motor speed controllers, are prevalent in today's power systems. These harmonics interfere with sensitive electronic equipment and cause unnecessary losses in electrical equipment. Active power filters were initially proposed by Sasaki and Machida (Sasaki and Machida 1971) as a means of removing current harmonics. An active power filter uses a switching inverter to produce harmonic compensating currents. It is only with the recent advances in semiconductor technology that high-speed, high-power switching devices suitable for constructing active power filters have become available (Duke and Round 1993, Akagi 1996).

Typical three-phase rectifier currents drawn by a variable speed motor drive are shown in Figure 1(a) with the frequency spectrum in Figure 1(b). This particular load draws odd harmonic frequencies with the dominant harmonics being the 5<sup>th</sup>, 7<sup>th</sup>, 11<sup>th</sup> and 13<sup>th</sup>. The fundamental component of the supply current is shown, since this is the waveform that the power system will supply after compensation.

Figure 2 is a single line representation of a three-phase active filter system.  $I_L$  is the load current drawn by the non-linear load and it is sensed by a current transducer. The resulting signal,  $I'_L$ , is fed into the digital signal processor (DSP) that performs harmonic isolation. The 'Harmonic Isolator' separates the harmonic current signal from the fundamental component of the load current signal so a compensating current can be calculated. The compensating current signal,  $I'_C$ , is the inverse (a 180° phase shift) of the harmonic current signal and it is used to control a three phase inverter so the appropriate compensating current,

$I_C$ , is injected into the power system. This cancels the harmonics drawn by the non-linear load, leaving the resulting supply current,  $I_S$ , sinusoidal.

### 1.2 Hysteresis Current Control

Active filters produce a nearly sinusoidal supply current by measuring the harmonic currents and then injecting them back into the power system with a  $180^\circ$  phase shift. A controlled current inverter is required to generate this compensating current. Hysteresis current control is a method of controlling a voltage source inverter so that an output current is generated which follows a reference current waveform. This method controls the switches in an inverter asynchronously to ramp the current through an inductor up and down so that it tracks a reference current signal. Hysteresis current control is the easiest control method to implement (Brod and Novotny 1985). One disadvantage is that there is no limit to the switching frequency, but additional circuitry can be used to limit the maximum switching frequency (Malesani *et al* 1996).

A hysteresis current controller is implemented with a closed loop control system and is shown in diagrammatic form in Figure 3(a). An error signal,  $e(t)$ , is used to control the switches in an inverter. This error is the difference between the desired current,  $i_{ref}(t)$ , and the current being injected by the inverter,  $i_{actual}(t)$ . When the error reaches an upper limit, the transistors are switched to force the current down. When the error reaches a lower limit the current is forced to increase. The minimum and maximum values of the error signal are  $e_{min}$  and  $e_{max}$  respectively. The range of the error signal,  $e_{max} - e_{min}$ , directly controls the amount of ripple in the output current from the inverter and this is called the Hysteresis Band. The hysteresis limits,  $e_{min}$  and  $e_{max}$ , relate directly to an offset from the reference signal and are referred to as the Lower Hysteresis Limit and the Upper Hysteresis Limit. The current is forced to stay

within these limits even while the reference current is changing. The ramping of the current between the two limits is illustrated in Figure 3(b).

The switching frequency is altered by the width of the hysteresis band, the size of the inductor that the current flows through ( $L$  in Figure 3(a)) and the DC voltage applied to the inductor by the inverter. A larger inductance will yield a smaller  $\frac{di}{dt}$  for a given voltage and so the slope of the sawtooth waveform in Figure 3(b) will be less.

### *1.3 Digital Control of Inverter Current*

The active filter controller is implemented with a Digital Signal Processor (DSP). All calculations are made digitally and the desired compensating current is represented numerically inside the DSP. The power switches in an inverter can either be on or off, and thus can be considered to be digital. Therefore the inverter controller that interfaces the DSP to the inverter is ideally suited to be constructed from a digital circuit rather than the more common analogue implementation. The digital inverter controller calculates the hysteresis limits mathematically and performs the magnitude comparisons with digital logic. Traditional hysteresis current controllers perform these functions with analogue operational amplifiers and comparators. Laying an analogue circuit out on a printed circuit board takes a considerable amount of time and uses a large number of components, many of which require fine adjustment. Any changes to the design would result in the procedure being repeated. A Field Programmable Gate Array (FPGA) is a reprogrammable digital logic integrated circuit and allows modifications to the inverter controller to be made internally without any changes to the printed circuit board. An FPGA implementation is very compact because it is a single component and does not require a large number of support integrated circuits (Retif *et al.* 1993).

Other digital inverter controllers have been built with a DSP and programmable logic, usually erasable programmable logic devices (EPLD). One such example is that of Lee *et al.* (Lee *et al.* 1996) where space voltage vector control was implemented with a Texas Instruments TMS320C31 DSP and an EPLD. Other researchers have implemented a digital hysteresis current controller using the TMS320C31 DSP (Li *et al.* 1995). These inverter controllers operate with a low sampling and/or switching frequency of several kilohertz. This low switching frequency is not high enough to adequately track the active filter's compensating currents. A digital hysteresis current controller that can generate a high frequency switching signal suitable for an active filter by operating with a sampling rate of 260 kHz is presented and discussed in this paper.

## **2. Theory**

### *2.1 Active Power Filtering Requirements*

Active power filtering imposes design restrictions on the inverter that would not normally be present in other applications, for example, motor speed control. The main difference between these two applications is the maximum frequency of the current reference. An active power filter should at least be able to inject frequencies up to the 20th harmonic and ideally be able to compensate up to the 50th harmonic.

This high frequency operation limits the size of the injection inductor. When the inductance is too large the maximum rate of change of current will be too low to track the steep current changes that occur with high frequencies. The small inductances used mean that the rates of change of current will be high. High switching frequencies result and this causes large losses in the semiconductor switches. This also leads to increased levels of electromagnetic

interference and requires very high-speed comparisons of the actual current against the hysteresis limits (illustrated in Figure 3(b)).

## 2.2 Injection Inductor

The injection inductor must be small enough so that the injected current  $di/dt$  is greater than that of the reference current (the compensating current signal in the active power filter) for the injected current to track the reference. If Eqn. (1) describes the reference current at the highest frequency, the maximum  $di/dt$  can then be determined from Eqn. (2).

$$i(t) = A \sin(2\pi f t) \quad (1)$$

$$\max\left(\frac{di}{dt}\right) = A 2\pi f \quad (2)$$

In order to determine the maximum  $di/dt$  of the compensating current the  $di/dt$  of each harmonic component must first be calculated from its amplitude and frequency values. The overall maximum  $di/dt$  for the compensating current is therefore the highest individual  $di/dt$ . As an example the harmonic giving the highest  $di/dt$  is generally the third for single-phase rectifiers with capacitive loads, yet is the fifth for three phase rectifiers with inductive or capacitive loads.

From the standard inductor differential equation an expression for  $di/dt$  can be determined and is given by Eqn. (3) where  $\Delta V$  is the voltage across the inductor (assuming negligible resistance).

$$\frac{di}{dt} = \frac{\Delta V}{L} \quad (3)$$

The maximum inductance possible should be used in the inverter to give the lowest average switching frequency. This in turn reduces electromagnetic interference (EMI) and switching losses in the inverter. An expression for the maximum useable inductance is given by Eqn.

(4), where  $V_{DC}$  is the rail-rail DC voltage on the inverter and  $v_{\text{supply}}$  is the instantaneous power supply voltage.

$$L_{\text{max}} = \frac{\frac{1}{2}V_{DC} - v_{\text{supply}}}{\frac{di}{dt}_{\text{Reference(max)}}} \quad (4)$$

Brod and Novotny (Brod and Novotny 1985) present an expression for the maximum switching frequency of a hysteresis controller, and this is given in Eqn. (5), where  $h$  is the hysteresis limit, and so the hysteresis band,  $\Delta I$ , is equal to  $2h$ .

$$f_{\text{sw(max)}} = \frac{V_{DC}}{9hL} \quad (5)$$

### 2.3 Sampling Frequency

Hysteresis current control requires current feedback. The sensed current is compared to the hysteresis limits and the result of this comparison is used to control the switches in the inverter. In an analogue system the comparisons are made continuously and the current will be forced to stay within the hysteresis band at all times. With a digital controller, events happen at discrete intervals. The sensed current is digitised and the comparisons are made digitally. The current information is updated at the sampling frequency of the analogue to digital converter (ADC) that samples the current feedback. If this sampling frequency is too low there is a chance that the current will have exceeded the hysteresis limits by the time the comparison is made.

Figure 4 shows the results of a simulated inverter controller with two different sampling frequencies. The injected current is sampled at 5kHz in (a) and at 260kHz in (b). The hysteresis band,  $\Delta I$ , has been set to 0.8A in both cases. It can be seen that the current regularly exceeds the hysteresis band when the current feedback is sampled too slowly. The reference and the two hysteresis limits are shown as discrete samples in Figure 4(a) and (b). Once a

switching decision has been made the inverter switches are left unchanged until the next sample is taken. This new sample is used by the decision logic to determine the next switching state. The centre solid line in each figure is the current reference and the jagged solid line is the inverter's current output. Two dashed lines represent the hysteresis limits used for the simulation.

Once the injected current travels outside of the hysteresis limits it will continue to do so until the next sample is taken. It is only at this point that the transistors are set so the current is ramped in the opposite direction. The high speed sampling of 260kHz gives very good results, and with only 3.8 $\mu$ s between samples the current will not get far outside the hysteresis limits. Compare this with the case of 5kHz sampling, where the current is regularly outside of the hysteresis limits. The time between samples has extended to 200 $\mu$ s, leading to extremely large current excursions. The minimum sampling frequency needed to achieve an acceptable overshoot is a function of the injection inductance used and the voltage applied across the inductance. Each of these affects  $\frac{di}{dt}$ , and therefore the level of current overshoot.

The smaller the injection inductor, the greater the  $\frac{di}{dt}$ , and this will increase the current overshoot. The worst case is when the current is just inside the hysteresis band when the comparison is made. The current will then continue on past the limit and will only reverse direction at the next sampling point. Eqn. (6) gives the maximum current overshoot  $\Delta i_{Over}$  for an inverter with a DC voltage  $V_{DC}$  injecting current into an inductance  $L$  with a sampling frequency of  $f_{Sample}$ , assuming that  $v_{Supply} = 0$ . Acceptable current waveforms are achievable by choosing the sampling frequency so that the overshoot is kept to 5-10% of hysteresis band,  $\Delta I$ . This keeps the current ripple reasonably close to the design value for a traditional analogue hysteresis current controller.

$$\Delta i_{Over} = \frac{\frac{1}{2} V_{DC}}{L} \frac{1}{f_{Sample}} \quad (6)$$

### 3. Simulation

The operation of the proposed digital hysteresis current controller has been modelled using Simulink and MATLAB. A single-phase model was developed since the three phases of the inverter are able to operate independently. A neutral connection is provided and this prevents the situation arising where the hysteresis band can double due to three phase interactions (Brod and Novotny 1985).

To get the best possible simulation of a real digital hysteresis current controller the currents were quantised and sampled. This gives the simulated controller the same dynamic characteristics as a controller implemented in an FPGA. The hysteresis controller makes switching decisions based on the reference current signal and the current feedback. The switching signals are used to control a model of a three-phase inverter that in turn produces a three-phase voltage output. The voltage is applied across the injection inductor model, which through the use of differential equations determines the current that flows through the inductor. This injection current is the output from the simulation and is recorded for further analysis.

This digital inverter controller is intended for use in an active filter, and so a sample compensating current, shown in Figure 5(a), was generated. The fundamental frequency is 50Hz and the injection inductance is 4mH. The compensating current is scaled for an overall load current of  $0.71A_{RMS}$  and the hysteresis band is 0.2A. Figure 5(b) shows the frequency spectrum of the current in Figure 5(a). The two prominent frequency components at 250Hz and 350Hz are the harmonics present in the reference signal. The concentration of signal at 13.5kHz is the high frequency switching signal from the inverter. The maximum expected

frequency in the inverter output as calculated by Eqn. (5) is 16.7kHz and this agrees with the frequency spectrum in Figure 5(b). The unwanted frequency components can be filtered by an LC low pass filter because they are so far removed from the frequency band of interest, which is limited to 2.5kHz (50<sup>th</sup> harmonic at 50 Hz).

## **4. Inverter Controller Implementation**

### *4.1 System Diagram*

The digital inverter controller interfaces the digital signal processor to the three-phase inverter. Figure 6 shows the inverter system with the controller, the power inverter and current feedback. A current sensor and transimpedance amplifier convert the high current output of the inverter to a voltage suitable for digitising by the ADC. The reference current from the DSP and the digitised injection current are transmitted digitally to the FPGA. Switching decisions are made by the FPGA that control the output voltage of the inverter. The voltage applied to the inductor causes a current to flow into or out of the power system.

Figure 7 expands upon the inverter controller, highlighting the internal blocks needed for hysteresis current control. The controller is completely digital and implemented inside the FPGA.

### *4.2 Inverter Controller Parameters*

There are a few parameters to be selected for a digital hysteresis controller that are not required for an analogue controller. Firstly, the resolution of the currents must be specified. The intended active power filter will be working with load currents up to 400A<sub>Peak</sub> and a current precision of 0.2A is required. This gives 4000 points over the full scale of the current (from -400A to +400A). A twelve-bit integer has 4096 possible values and can be used to represent the load current with the desired precision. The DSP will be working with 12-bit

integers internally and will represent the compensating current as a twelve-bit number. To aid the comparison of values digitally the current feedback will be digitised with a twelve-bit analogue to digital converter (ADC).

Secondly, the update frequency of the reference value from the DSP and the sampling frequency of the current reference ADC must be selected. A fast sampling frequency is required for this ADC to ensure that the current ramps in the opposite direction as soon as a hysteresis limit is reached. For a  $70A_{RMS}$  compensating current a suitable value of  $h$  is 2A to 5A. Any current overshoot will add to this and should be minimal and so a suitable limit for current overshoot is 1A. The maximum inductance that can be used for an active power filter injecting  $60A_{RMS}$  of the 5th harmonic into a  $230V_{rms_{SLN}}$  supply with a bus voltage of  $800V_{DC}$  is  $670\mu H$ . To ensure the current overshoot does not exceed 1A the sampling frequency must be at least 133kHz, as given by Eqn. (6). A sampling frequency of 260kHz has been selected for this inverter controller. This is fast enough to reduce the level of current overshoot with the inductor that will be used.

#### *4.3 The FPGA Controller Implementation*

A Xilinx XC4010E FPGA was used to implement the digital hysteresis current controller. This FPGA contains 400 configurable logic blocks (CLBs) that are arranged in a 20 x 20 matrix. Each CLB contains two D-type flip-flops and three combinational logic function generators. The functionality of each CLB is customised during configuration at power up. The inputs and outputs of the CLB connect to programmable interconnect resources that extend through out the entire FPGA. Around the perimeter of the FPGA there are user-configurable blocks that provide the logic interface between the external package pins and the internal logic. The Xilinx XC4010E FPGA contains a total of 1120 flip-flops and is approximately equivalent to 10000 logic gates (Xilinx 1996).

The harmonic isolator is implemented in a Texas Instruments TMS320C30 32-bit floating point DSP. The DSP communicates with the FPGA through its synchronous serial port with an 8MHz clock. A 12-bit serial ADC is used on each phase for the current feedback with a sampling frequency of 260kHz. This is a significant improvement over the minimum sampling requirement of 133kHz. Serial communication reduces the number of input connections to the FPGA but increases the internal decoding logic.

The internal logic implemented in the FPGA is shown in Figure 7. The serial data stream from the ADC is clocked into a shifter register contained in the ADC Interface block. Once all of the 12-bits are clocked in the data is then stored in a 12-bit register. This 12-bit value represents the instantaneous inverter current for a single phase. Three 12-bit values are required for a three-phase inverter. Similarly for the DSP interface, the serial current reference signals and hysteresis band value are clocked into a shift register and stored in separate registers. The hysteresis band value is added and subtracted from each current reference signal by two 12-bit adder/subtractors to generate the upper and lower hysteresis limits. Two 12-bit two's-complement magnitude comparators check the instantaneous current value against these limits. The outputs of the two comparators provide a signal that indicates whether the current is outside the hysteresis band. A set-reset flip-flop then determines the appropriate switching pattern to drive the current in the appropriate direction through the injection inductor. A small  $2\mu\text{s}$  delay is added to the switching signals by a small finite state machine counter to ensure that the switching devices in each inverter leg are not on simultaneously. The three-phase digital implementation of the current controller in the Xilinx XC4010E FPGA uses 37% of its resources.

## 5. Experimental Results

A small-scale inverter is used for verifying the operation of the digital current controller. The inverter operates off a 60V DC bus and the inverter has a peak current rating of 10A. The experimental implementation of a digital hysteresis current controller was tested with sinusoidal and harmonic current outputs.

### 5.1 Inverter Operation

The DSP is programmed to generate a sinusoidal reference signal with a fundamental frequency of 36Hz and a magnitude of 6A. The DSP also sets the current controller to generate the output current with a hysteresis band of 0.1A. The upper plot of Figure 8(a) shows the frequency spectrum of the current output. There is a large peak near 0Hz representing the fundamental frequency. The asynchronous nature of the hysteresis current controller is shown by the band of frequencies at 4.7kHz. The lower plot in Figure 8(a) shows just over one cycle of the output current shown in the time domain. The current ripple is small in comparison to the overall magnitude of the current and that there are no significant current overshoots. Overshoots have occurred and Figure 8(b) shows one of these in one of the positive half cycles of current. The circle 1.2ms to the left of centre shows where the current has deviated from the reference by twice the design limit for the hysteresis controller. This was due to the inverter controller sampling the injection current when it was just inside the hysteresis limit. The hysteresis band in Figure 8(b) is relatively constant over the half cycle. This indicates that the sampling frequency is high enough as there are no large current overshoots.

A sample compensating current that would result from a three-phase bridge rectifier with capacitive smoothing was generated artificially by the DSP. The fundamental frequency is 50Hz and the overall output current is  $0.71A_{RMS}$ , with a hysteresis band of 0.2A. The

waveform illustrated in Figure 9 is the time domain representation of the output current. The  $\frac{di}{dt}$  of the output current has been increased by reducing the injection inductance so the current can follow the higher frequency reference. This gives more switching operations at the top of each current peak when the slope is near zero. This is seen in Figure 9 as increased current noise at the top of the peaks. The experimental waveform in Figure 9 is very similar to that generated by simulation and shown in Figure 5.

### 5.2 Average Switching Frequency

The hysteresis current controller ideally has a constant current ripple,  $\Delta i$ , but no defined switching period  $\Delta t$  (Brod and Novotny 1985). The maximum switching frequency occurs in a hysteresis controlled inverter when the gradient of the reference current is near zero, as illustrated in Figure 3. To test the validity of Equations (5) and (6) the inverter was operated with a zero voltage reference to make the average inductor current zero. Table 1 summarises the measurements taken. It can be seen that the calculated and observed results are very close from where  $h = 0.2A$ .

Further tests were conducted with a single 60Hz sinusoid injected into the inductor. Table 2 shows the frequency and magnitude of the switching frequency with respect to the magnitude of the 60Hz fundamental. The entries where the hysteresis limit is 10% of the peak current are highlighted.

The results in Table 2 show that the magnitude of the switching noise is, on average, 4% of the fundamental current when the hysteresis limit is one tenth of the reference current peak. The lowest level of switching noise was with  $h = 0.1A$ ,  $I_P = 6.0A$  and was 0.5% of the fundamental and is an improvement over the 3% magnitude obtained with  $h = 0.6A$ . The

average switching frequency is shown by the results in Table 2 to depend only upon  $h$ , as is expected from Eqn. (5).

### *5.3 Noise Immunity*

One benefit of digital control is that the current reference is transmitted serially from the DSP to the inverter controller. It was predicted that this would enhance the controller's ability to withstand electromagnetic interference (EMI). The susceptibility to EMI of this prototype inverter controller was tested by operating a 146.475MHz radio transmitter at a variety of distances from the controller. Even though oscilloscope waveforms showed increased noise on the voltage signal feeding to and from the FPGA, there was minimal disturbance to the current waveform from the inverter. Disturbance only occurred when the tip of the transmitting antenna was touching the Xilinx FPGA. The inverter failed to operate once the transmitter was stopped, and only started again when the DSP updated the reference and hysteresis limits. This suggests that a register change occurred in the Xilinx FPGA due to the high electrical fields present (about 100-200V/m). This level of EMI would seldom be found except near radio transmitters. It can be assumed that the digital inverter controller itself is not susceptible to EMI.

The one weakness in the system is the analogue to digital converter (ADC) used for digitising the current feedback. The input to the ADC does show noise in the presence of EMI and so great care must be taken to ensure that this device and its associated analogue circuitry are well shielded.

### *5.4 Current Overshoot*

The sampling frequency for the current feedback is fixed at 260 kHz, and therefore some current overshoot will occur. The current swing was measured while the switching frequency tests were being performed. For this test,  $L = 9\text{mH}$ ,  $V_{DC} = 60\text{V}$  and  $f_{Sample} = 260\text{ kHz}$ . From

Eqn. (6) the value of overshoot,  $\Delta i_{Over}$ , is 16mA. Table 3 summarises the level of overshoot for six values of the hysteresis limit  $h$ .

Whilst the predicted maximum overshoot is independent of the hysteresis limit,  $h$ , this is not so for the experimental results. Measuring small currents is difficult and the input to the current feedback ADC has a noticeable level of noise. This will affect the inverter controller's ability to determine accurately when the current has exceeded the hysteresis band. It is expected that by dealing with larger currents the effect of noise on the analogue circuitry will be reduced.

## **6. Conclusion**

A fully digital hysteresis current controller has been designed and implemented in a Xilinx Field Programmable Gate Array. This completely digital controller makes the switching decisions for hysteresis current control. The theoretical performance of a digital hysteresis controller has been presented. The inverter controller has been tested on a small-scale inverter, with experimental results providing performance data and verification of the accuracy of the simulation model used.

The digital implementation of a hysteresis current controller was successful and performed as expected. High levels of immunity to EMI make this type of current controller very promising for use in full size high frequency switching inverters. A digital interface makes connection to an active filter controller straightforward and robust. The controller is adaptable for use in any application requiring current control of a voltage source inverter and is not limited to active filtering.

## **Acknowledgments**

Financial support for David Ingram was provided by the Metalect Industries (NZ) Ltd Power Electronics Scholarship and by the Telecom Corporation of New Zealand Fellowship in Telecommunications Engineering.

## References

- AKAGI, H., 1996. New Trends in Active Filters For Power Conditioning. IEEE Transactions on Industry Applications, 32, 1312-1322.
- BROD, D.M., NOVOTNY, D.W., 1985. Current Control of VSI-PWM Inverters. IEEE Transactions on Industry Applications, IA-21, 562-570.
- DUKE, R.M., ROUND, S.D., 1993. The Steady-State Performance of a Controlled Current Active Filter. IEEE Transactions on Power Electronics, 8, 140-146.
- LEE, H., SUH, B.S., HYUN, D.S., 1996. A Novel PWM Scheme for a Three-Level Voltage Source Inverter with GTO Thyristors. IEEE Transactions on Industry Applications, 32, 260-268.
- LI, Z., JIN, H., JOOS, G., 1995, Control of Active Filters Using Digital Signal Processors. 21st International Conference on Industrial Electronics, Control and Instrumentation (IECON '95) (Orlando, USA), 1, 651-655.
- MALESANI, L., ROSSETTO, L., TOMASIN, P. ZUCCATO, A., 1996. Digital Adaptive Hysteresis Current Control With Clocked Commutations and Wide Operating Range. IEEE Transactions on Industry Applications, 32, 316-325.
- RETIF, J.M., ALLARD, B., JORDA, X. PEREZ, A., 1993, Use of ASICs in PWM Techniques for Power Converters. 19th International Conference on Industrial Electronics, Control and Instrumentation (IECON '93) (Maui, Hawaii, USA), 2, 683-688.
- SASAKI, H., MACHIDA, T., 1971. A New Method to Eliminate AC Harmonic Currents by Magnetic Flux Compensation - Considerations on Basic Design. IEEE Transactions on Power Apparatus and Systems, PAS-90, 2009-2019.
- XILINX, 1996, The Programmable Logic Data Book (San Jose, California, USA: Xilinx).

Table 1 Maximum inverter switching frequency.

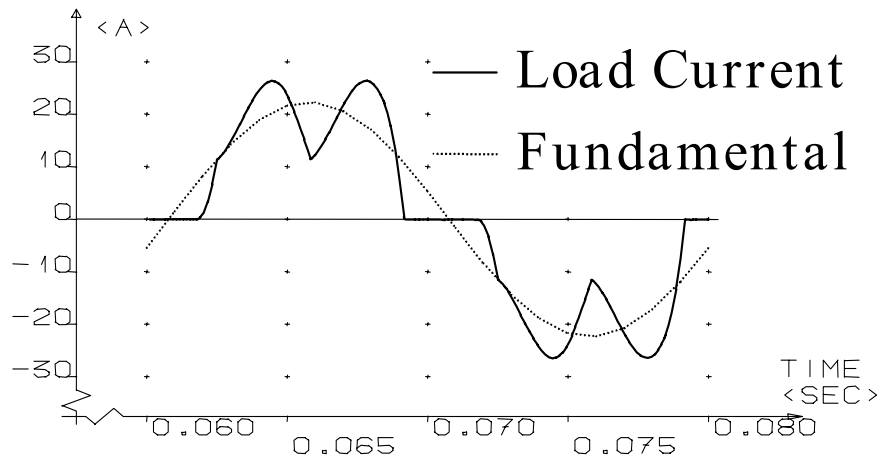
$h$ (A) ( $\frac{1}{2}\Delta I$ )	Max Frequency (kHz)	
	Calculated	Observed
0.1	7.4	5.9
0.2	3.7	3.6
0.3	2.5	2.6
0.4	1.9	1.8
0.5	1.5	1.5
0.6	1.2	1.3

Table 2 Relative magnitude and average inverter switching frequency.

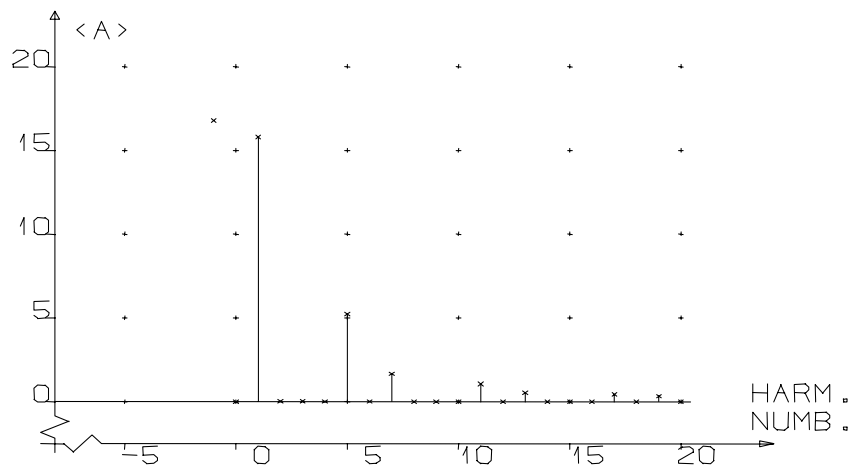
$I_P$ (A)	$h$ (A)					
	0.1	0.2	0.3	0.4	0.5	0.6
1.0	7.2% 7.1kHz	15.7% 3.7kHz	21.4% 2.5kHz			
2.0	2.5% 7.7kHz	6.1% 3.5kHz	10.2% 2.5kHz			
3.0	1.8% 7.8kHz	2.2% 3.7kHz	3.6% 2.4kHz			
4.0	0.8% 7.7kHz	1.8% 3.7kHz	2.3% 2.4kHz	3.3% 1.8kHz		
5.0	0.7% 7.7kHz	1.3% 3.6kHz	1.8% 2.4kHz	2.3% 1.8kHz	3.7% 1.4kHz	
6.0	0.5% 7.7kHz	0.6% 3.6kHz	1.0% 2.4kHz	1.8% 1.7kHz	2.7% 1.3kHz	3.1% 1.0kHz

Table 3 Current overshoot from the hysteresis band.

$h$ (A) ( $\frac{1}{2}\Delta I$ )	Overshoot (mA)	
	Predicted	Actual
0.1	13	28
0.2	13	40
0.3	13	74
0.4	13	76
0.5	13	65
0.6	13	60



(a)



(b)

Figure 1 Load current for a three-phase bridge rectifier in (a) the time domain and (b) the frequency domain.

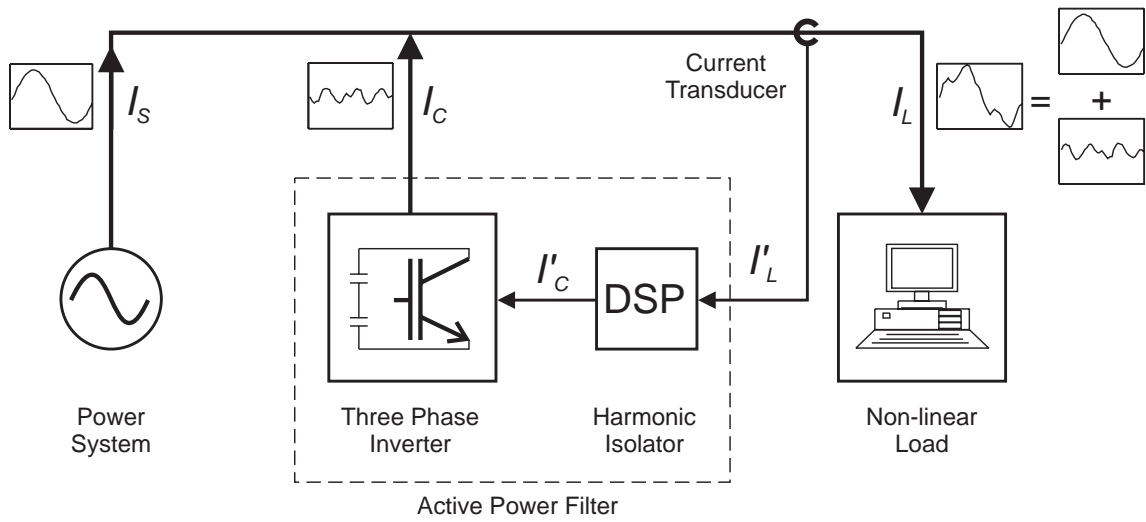
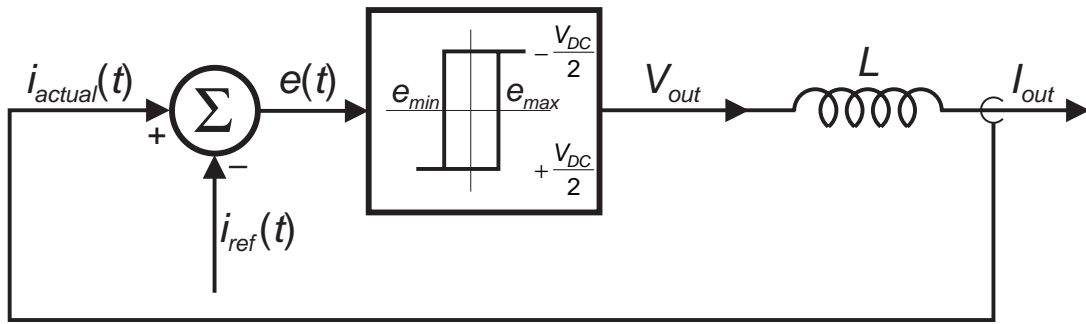
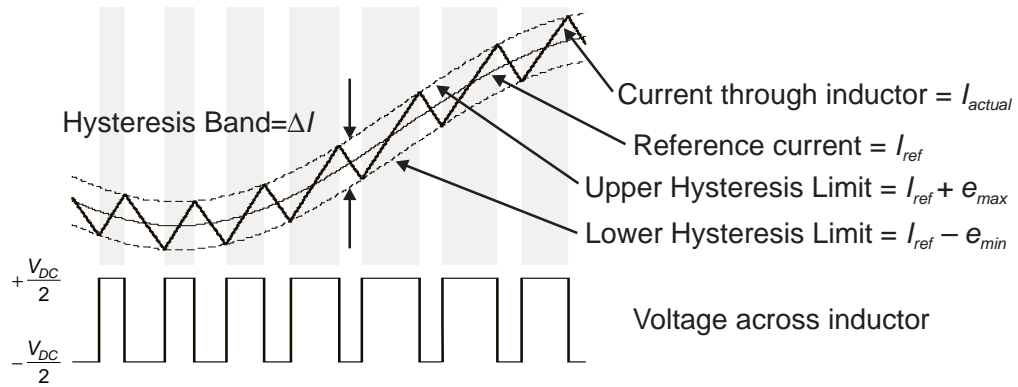


Figure 2 Single line diagram of an active filter.

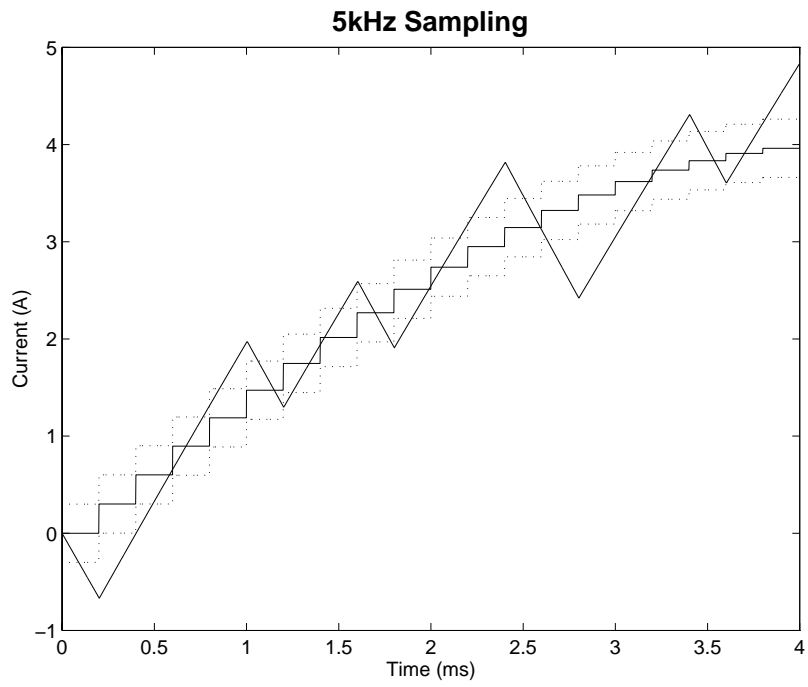


(a)

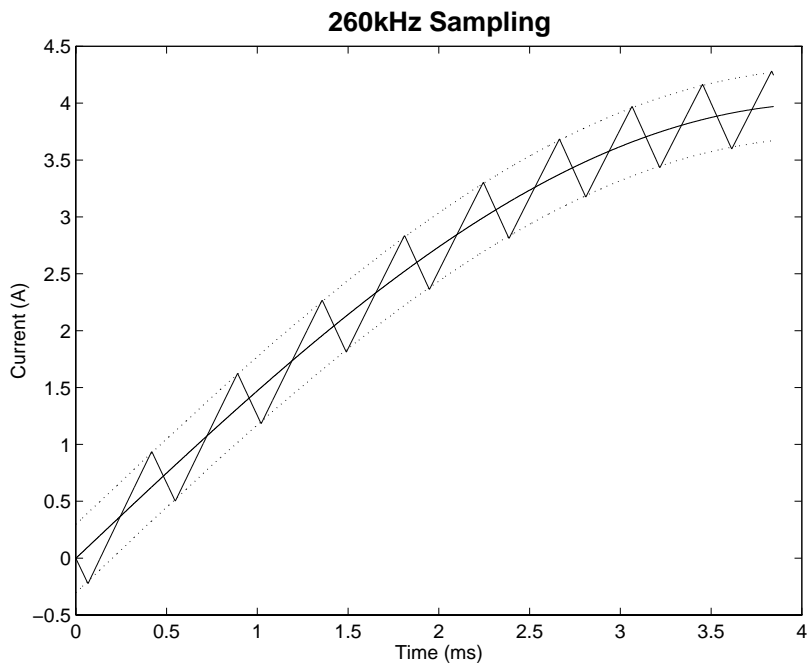


(b)

Figure 3 Hysteresis current controller (a) block diagram (b) operational waveform.

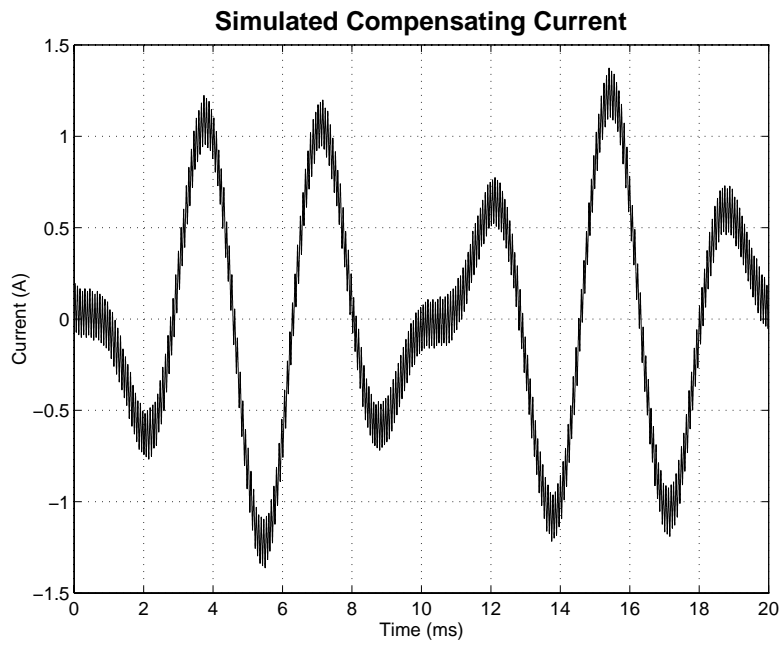


(a)

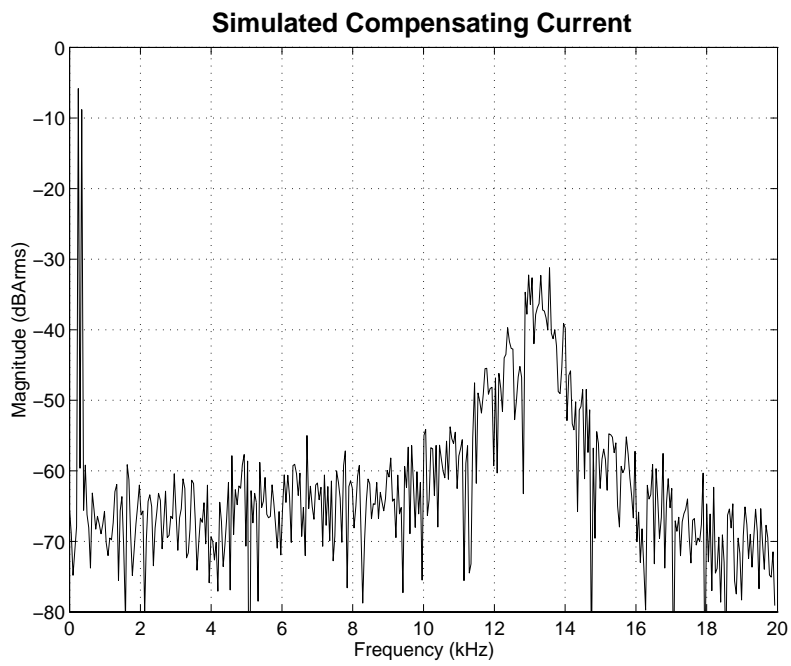


(b)

Figure 4 A higher sampling frequency reduces the level of current overshoot from the hysteresis limits.



(a)



(b)

Figure 5 Simulated compensating current output from Simulink.

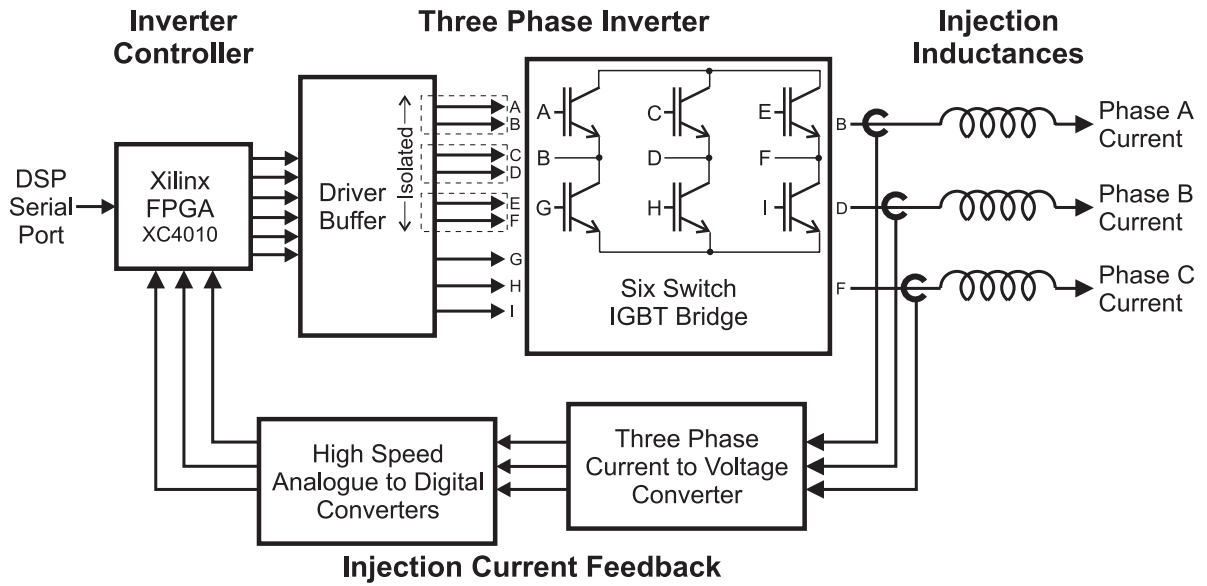


Figure 6 System diagram of the inverter and controller.

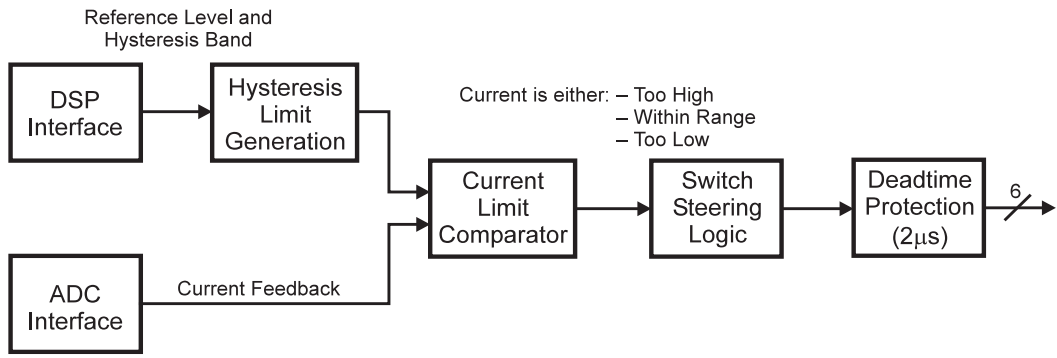
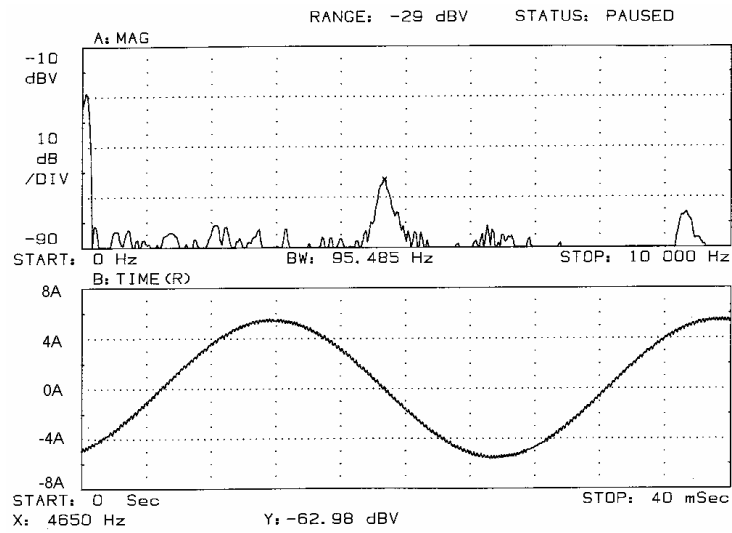
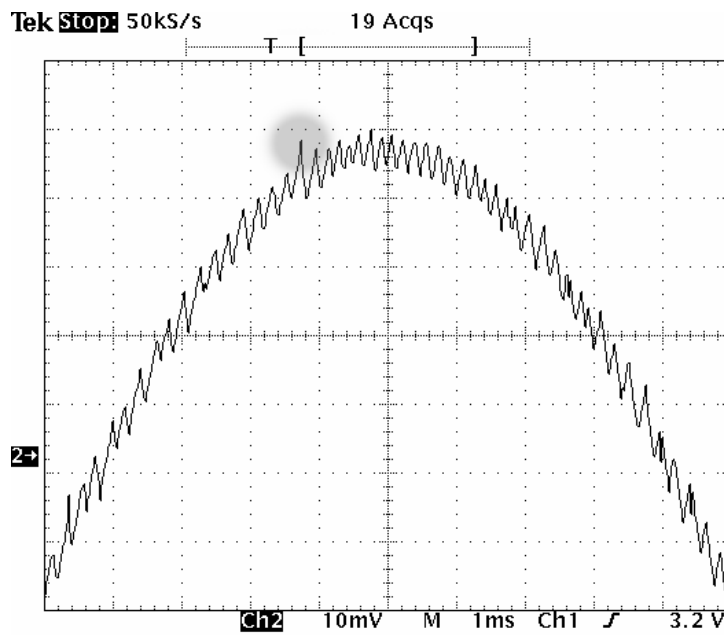


Figure 7 Block diagram of the inverter controller.



(a)



(b)

Figure 8 Sinusoidal current outputs from the digitally controller inverter of (a) the time and frequency domain, and (b) close up detail of the hysteresis.

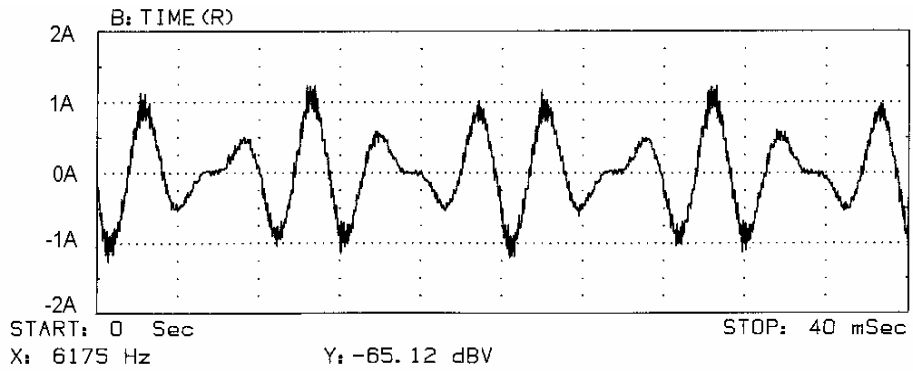


Figure 9 Compensating current output from the inverter.